Supplemental Figures

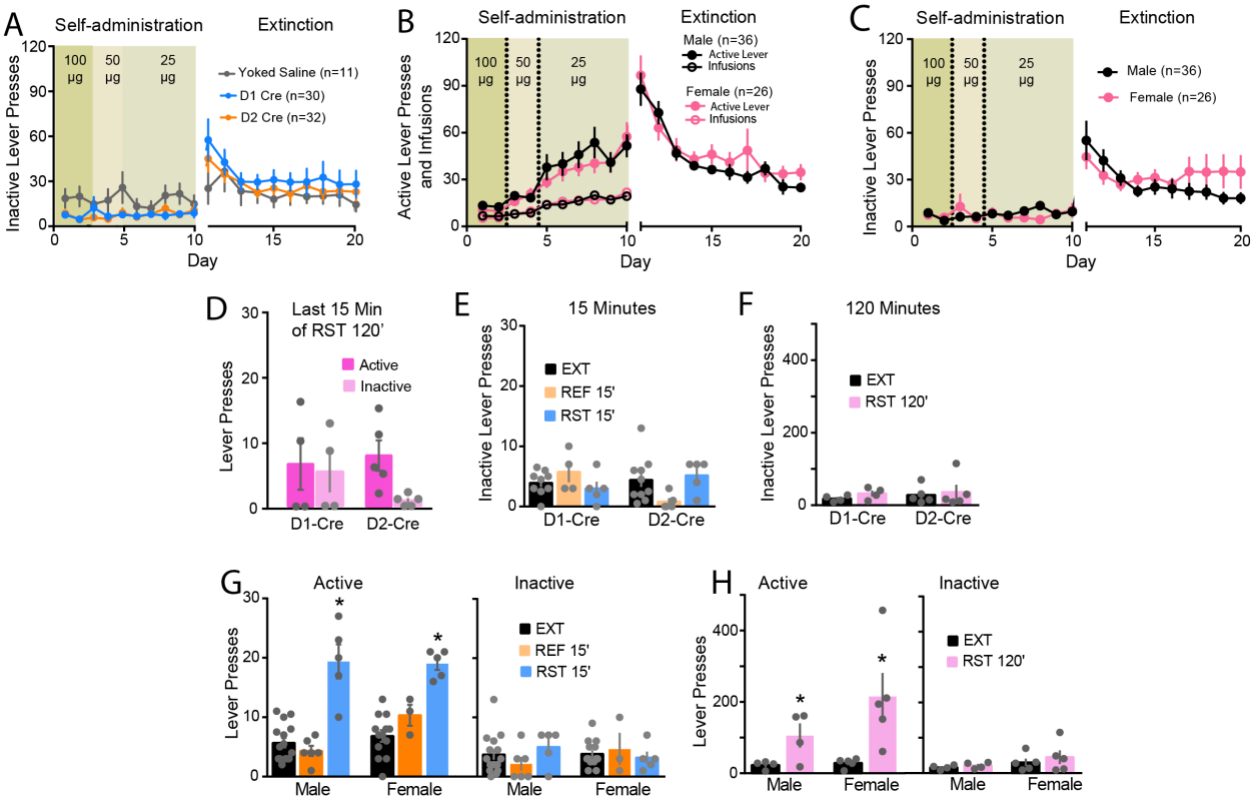

Supplemental Figure 1. Heroin self-administration and behavioral tests in D1- and D2-Cre rats. A) Time course of inactive lever pressing in D1- and D2-cre animals during heroin self-administration and extinction. No significant differences were found between yoked saline and both D1- and D2-cre rat genotypes during self-administration and extinction (2-way ANOVA; treatment $F_{(2,60)}$=0.24, p=0.791; time $F_{(19,1140)}$=8.61, p<0.001; interaction $F_{(38,1140)}$=1.27, p=0.130). No difference in inactive lever presses between D1-cre and D2-cre rats trained to self-administer heroin (2-way ANOVA; genotype $F_{(1,52)}$=0.42; p=0.519; time $F_{(19,\ 988)}$=16.02; p<0.001; interaction $F_{(19,988)}$=0.50; p=0.964). **B)** Time course of active lever pressing for male and female animals during heroin self-administration and extinction. No differences were found in active lever pressing (2-way ANOVA; sex $F_{(1,52)}$=0.03; p=0.873; time $F_{(19,988)}$=18.43; p<0.001; interaction $F_{(19,988)}$=0.90; p=0.584) or infusions (2-way ANOVA; sex $F_{(1,\ 52)}$=0.03; p=0.862; time $F_{(9,468)}$=28.81; p<0.0001; interaction $F_{(9,468)}$=0.51; p=0.871). **C)** No difference in inactive lever presses between males and females during self-administration and extinction (2-way ANOVA; sex

$F_{(1,52)}$=0.15, p=.70), but an effect of time $F_{(19,988)}$=16.07; p<0.001), interaction $F_{(19,988)}$=1.70; p=0.031). **D)** No difference in active or inactive lever pressing during the last 15 min of the 120 min reinstatement session between genotypes (RM 2-way ANOVA; genotype $F_{(1,7)}$=0.42; p=0.535; lever $F_{(1,7)}$=2,88; p=0.133; interaction $F_{(1,7)}$=0.16; p=0.698). **E)** No difference in inactive lever presses during behavioral tests (2-way ANOVA; genotype $F_{(5,22)}$=2.16; p=0.096; test $F_{(1,22)}$=0.22; p=0.640; interaction $F_{(5,22)}$=1.37; p=0.273). **F)** No difference in inactive lever presses during 120 min RST (2-way ANOVA; genotype $F_{(1,7)}$=0.16, p=0.699; EXT/RST $F_{(1,7)}$=2.18, p=0.183, interaction $F_{(1,7)}$=0.16, p=0.699). **G)** Cue-induced reinstatement of heroin-seeking increased active lever presses over 15 mins similarly in male and female rats (2-way ANOVA; interaction $F_{(3,15)}$=16.48; p<0.001). No difference in inactive lever presses during behavioral tests (2-way ANOVA; sex $F_{(3,15)}$=0.93; p=0.448; $F_{(1,15)}$=0.50; p=0.490; interaction $F_{(3,15)}$=0.10; p=0.960). **H)** No difference in active lever pressing between sexes during 120 min RST (2-way ANOVA; sex $F_{(1,7)}$=1.76; p=0.227, EXT/RST $F_{(1,7)}$=13.05; p=0.009, interaction $F_{(1,7)}$=1.93; p=0.207). No difference in inactive lever pressing between sexes during 120 min RST (2-way ANOVA; sex $F_{(1,7)}$=1.33; p=0.288, EXT/RST $F_{(1,7)}$=1.92; p=0.208, interaction $F_{(1,7)}$=0.40; p=0.546) Each dot in a bar represents an animal. Data are shown as mean ± SEM.

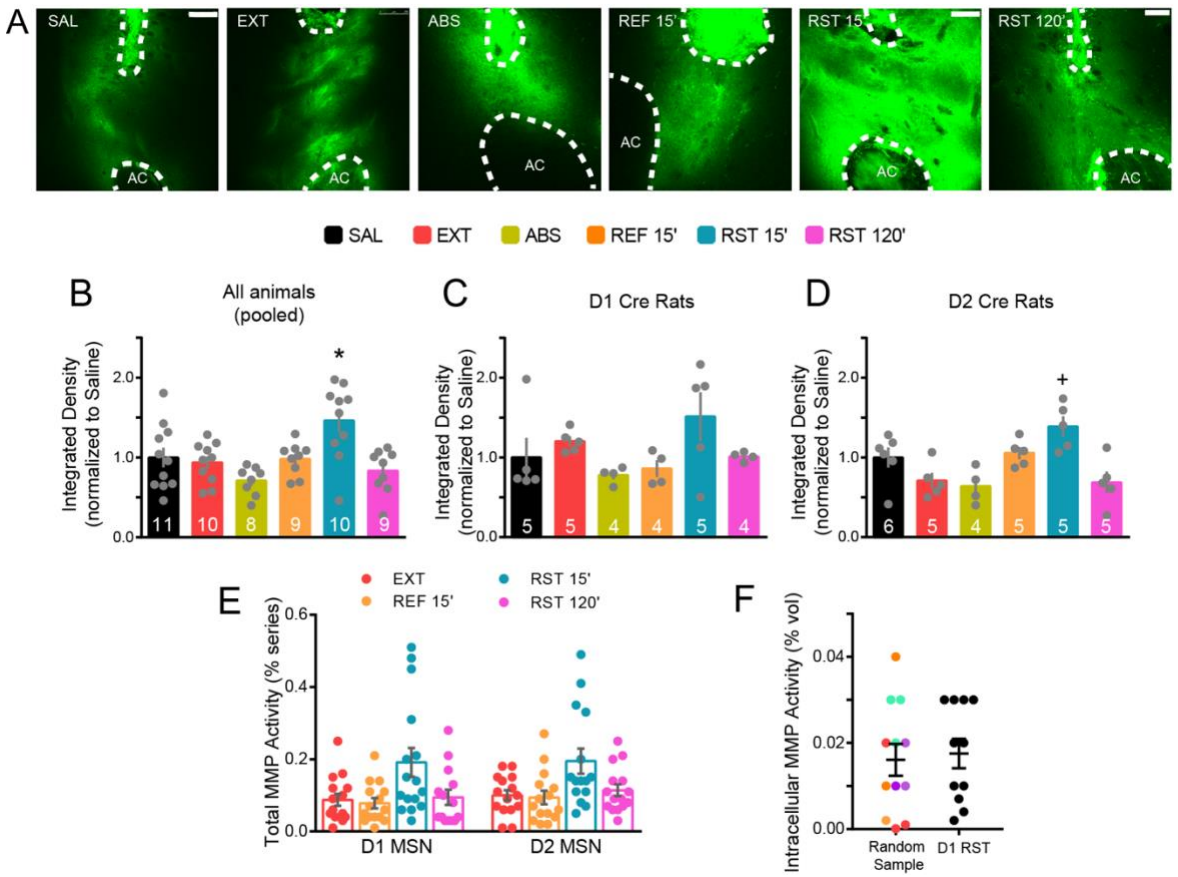

Supplemental Figure 2. MMP-2,9 activity in NAcore during withdrawn and heroin seeking behaviors. A) Representative micrographs of MMP-2,9 activity in NAcore following withdrawal (with or without extinction) and during behavioral seeking tests. **B)** Increased MMP-2,9 proteolytic activity in NAcore during transient heroin seeking compared to other behavioral groups in pooled analysis of both D1 and D2-cre rats (1-way ANOVA; $F_{(5,51)}$=5.802; p=0.0003). **C/D)** No difference in MMP activity across groups between D1 and D2 Cre rats (2-way ANOVA; effect of rat genotype, $F_{(1,\ 45)}$=2.781; p=0.1023; effect of treatment group, $F_{(5,\ 45)}$=5.349; p=0.0006; interaction, $F_{(5,\ 45)}$=1.259; p=0.2580. **D)** No difference in total MMP activity between D1- and D2-MSNs of EXT, REF 15', RST 15' and RST 120' groups (2-way ANOVA; effect of cell type, $F_{(1,\ 112)}$=0.577; p=0.4510; effect of group, $F_{(3,\ 112)}$=8.639; p=0.4510; interaction, $F_{(3,\ 112)}$=0.04193; p=0.9885. Three to four image series were quantified per animal. **F)** No difference in intracellular MMP activity between random sample of MSNs (same color-code=same animal; n=12) and D1 MSNs in RST group (n=12) (Unpaired t-test; $t_{(21)}$=0.286; p=0.7765). N in bars indicates number of animals with an average of four-seven NAcore slices/rat.

Data was normalized to its respective yoked saline mean. *$p<0.05$ comparing EXT, ABS, REF 15', RST 120' to RST 15' using Tukey post hoc test in pooled data. Data are shown as mean ± SEM. Scale bar=250 µm.

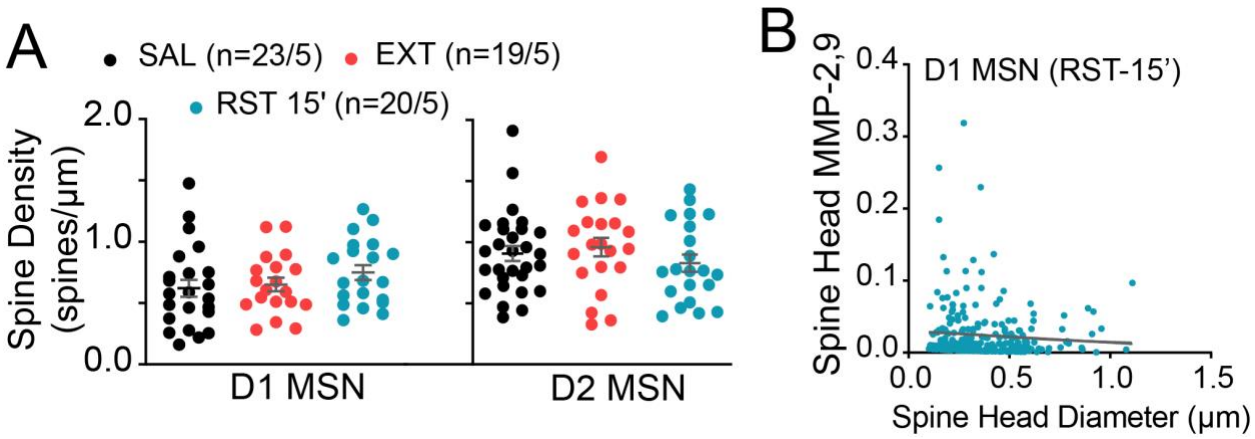

Supplemental Figure 3. Dendritic spine morphology: spine density in D1- and D2-MSNs. A) No difference in D1 MSN spine density across groups (nested 1-way ANOVA; $F_{(2, 12)}$=1.06; p=0.377). No difference in D2 MSN spine density across groups (nested 1-way ANOVA; $F_{(2, 13)}$=0.52; p=0.606). Data are shown as mean ± SEM. N represents number of neurons quantified over number of animals in each condition. **B)** No correlation between spine head diameter and the amount of MMP-2,9 adjacent to D1-MSN spine heads.

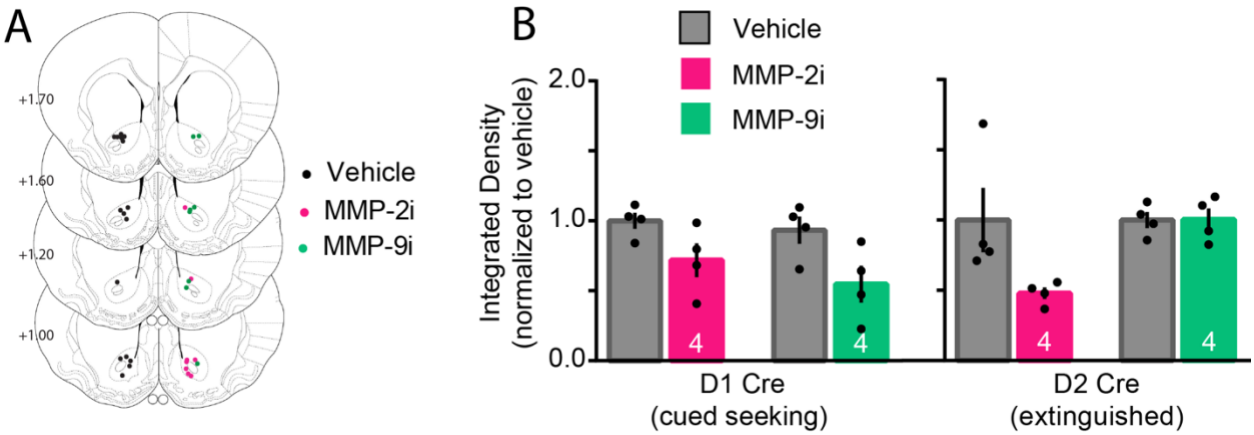

Supplemental Figure 4. Low-magnification MMP activity in NAcore following MMP-2 and -9 inhibition. A) Histological locations of microinjector tip for animals injected with vehicle (black) or MMP-2i (pink) or -9i (green). Animals received unilateral vehicle injection and contralateral injection of either MMP-2 or MMP-9 inhibitor. **B)** Neither MMP-2i and -9i injection (0.1 nmol each) decreased NAcore MMP activity during cued heroin seeking in D1 Cre rats (Paired t-test; MMP-2i: $t_{(3)}=3.00$, $p=0.058$; MMP-9i: $t_{(3)}=2.42$, $p=0.094$) or following extinction in D2 Cre rats (Paired t-test; MMP-2i: $t_{(3)}=2.323$, $p=0.1028$; MMP-9i: $t_{(3)}=0.0403$, $p=0.9704$). N in bars indicates number of animals with an average of four-seven NAcore slices/rat. Data were normalized to its respective vehicle and are shown as mean ± SEM.

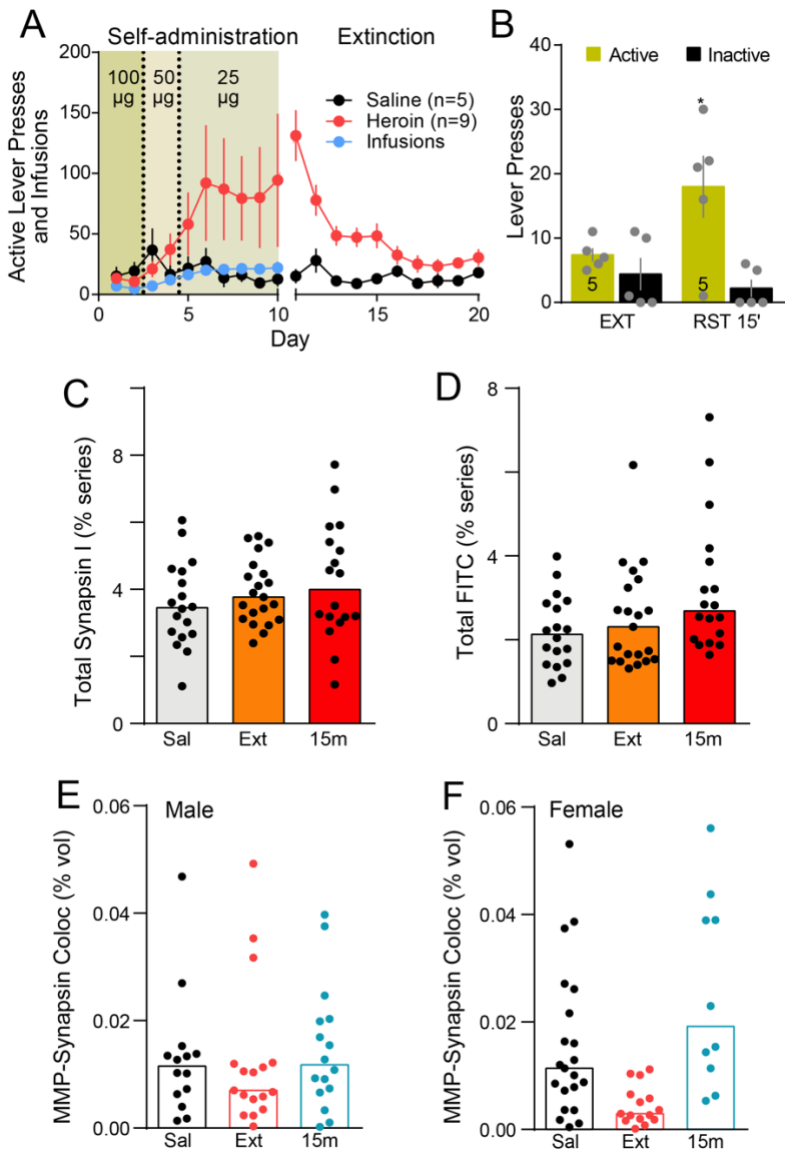

Supplemental Figure 5. Astroglia morphology: heroin self-administration behavior and total synapsin I and FITC quantifications. A) Time course of active lever pressing in wildtype animals during heroin self-administration and extinction. **B)** Cued heroin seeking induced significant active lever presses in rats (2-way ANOVA Inactive/Active $F_{(1,3)}$=467.3, p=0.0002; EXT/RST $F_{(1,3)}$=27.87, p=0.013; interaction $F_{(1,3)}$=12.71, p=0.038). **C)** No difference in total Synapsin I across groups; normalized to volume of image series (Kruskal-Wallis=1.61, p=0.448). **D)** No difference in total FITC/MMP activity between treatment groups; normalized to volume of image series (Kruskal-Wallis=5.21, p=0.074). Three to six image series were quantified per animal. N in bars indicates number of animals. Behavioral data are shown as mean ± SEM. *p<0.05 compared to inactive using

Bonferroni post hoc test. **E,F)** No sex differences observed for MMP-Synapsin I colocalization quantification (2-way ANOVA; effect of group $F_{(1,82)}$=7.67, p=0.007; effect of sex $F_{(2,82)}$= 1.38, p=0.259; interaction $F_{(2,82)}$=1.15, p=0.323). Astroglia quantification data are shown as median.

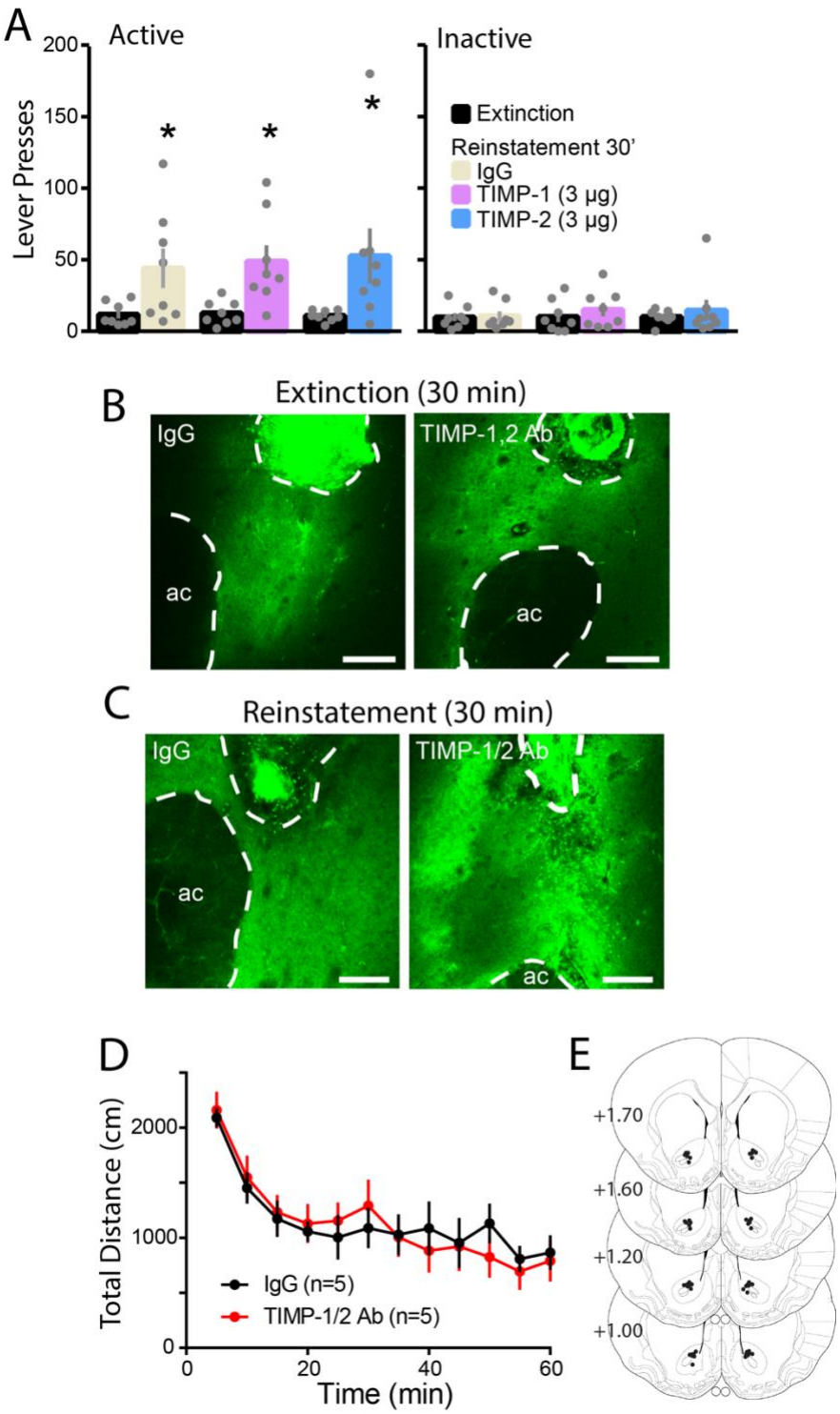

Supplemental Figure 6. Pharmacological TIMP-1 and -2 inhibition control experiments. A) No difference in cued heroin seeking between IgG or TIMP-1 or TIMP-2 antibody administration in NAcore (n=8; 2-way ANOVA; effect of treatment $F_{(2, 14)}$=0.1720; p=0.8437; EXT/RST $F_{(1, 7)}$=9.607, p=0.0173; interaction $F_{(2,14)}$=0.2145;

p=0.8096). No difference in inactive lever presses during cue-induced heroin seeking after IgG or TIMP-1 or -2 antibody microinjection (2-way ANOVA; effect of treatment $F_{(2,14)}$=0.1827; p=0.8350; EXT/RST $F_{(1,7)}$=1.818; p=0.2196; interaction $F_{(2,14)}$=0.1743; p=0.8419). **B)** Representative fluorescent micrographs of NAcore *in vivo* MMP activity in refraining controls and TIMP-1,2 antibody-treated animals. Injection track and anterior commissure masked out (dashed line). **C)** Representative fluorescent micrographs of NAcore *in vivo* MMP activity in reinstating IgG and TIMP-1,2 antibody-treated animals. Injection track and anterior commissure masked out. **D)** Open field locomotor activity showed no difference in total distance (cm) traveled between IgG and TIMP-1,2 antibody-treated animals (2-way ANOVA; $F_{(1,4)}$=24.09; p=0.4329). **E)** Histological locations of microinjector tip for animals injected with IgG (6 µg/ml) or combined TIMP-1,2 antibody (6 µg/ml) (black) in NAcore. Data are shown as mean ± SEM. *p<0.05 compared to extinction.

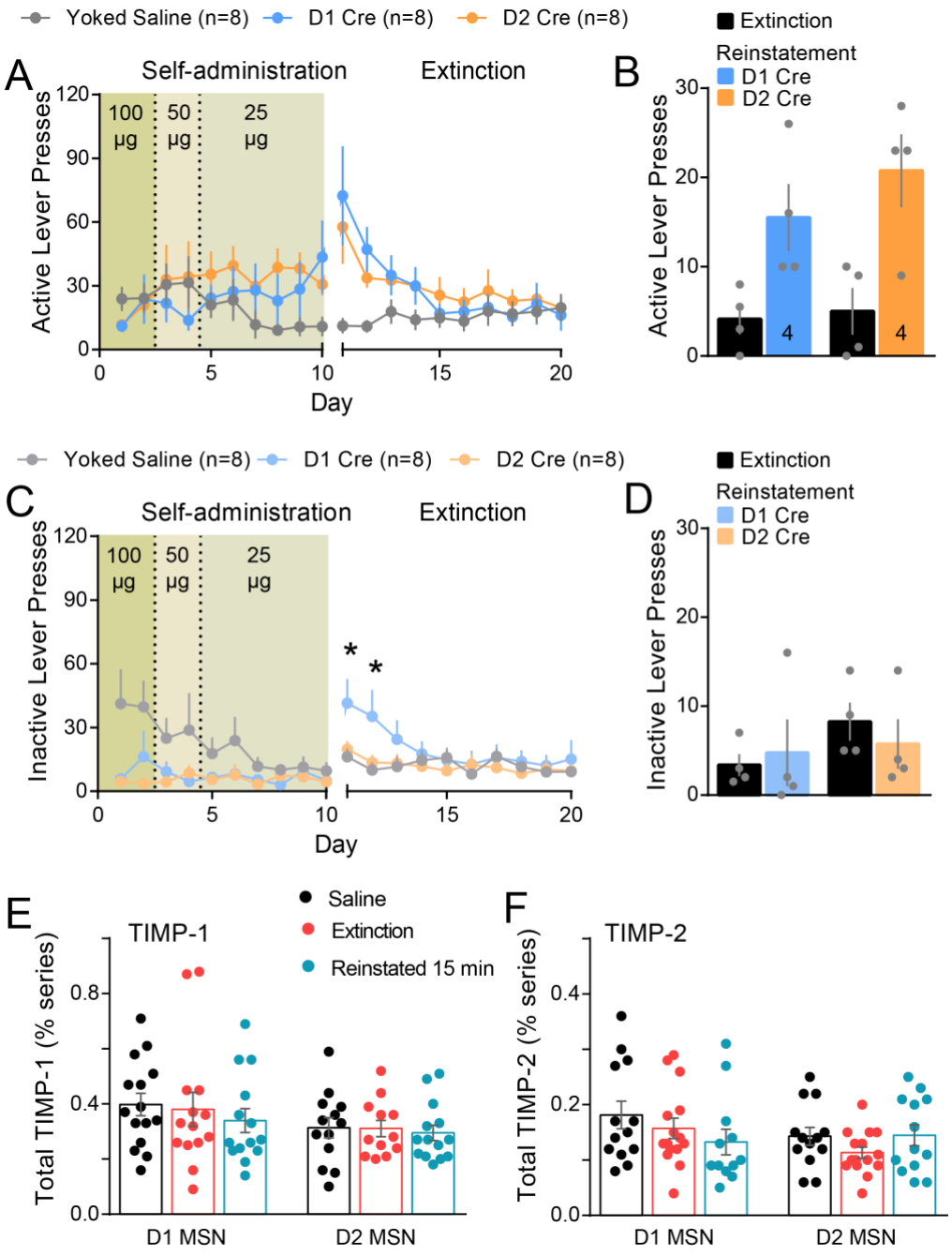

Supplemental Figure 7. D1- and D2-Cre heroin self-administration and reinstatement behavior and total TIMP-1 and -2 quantification. A) Time course of active lever pressing in yoked saline and D1- and D2-cre animals during heroin self-administration and extinction. No difference in active lever presses between D1-cre and D2-cre rats trained to self-administer heroin (2-way ANOVA; effect of genotype $F_{(1,14)}=0.3738$; $p=0.6820$; effect of time $F_{(19,266)}=3.704$; $p<0.0001$; interaction

$F_{(19,266)}$=0.6698; p=0.8474). **B)** Cue-induced reinstatement of heroin-seeking increased active lever presses over 15 mins similarly in D1- and D2-cre rats (2-way ANOVA; effect of genotype $F_{(1,6)}$=0.5776; p=0.4761; EXT/RST $F_{(1,6)}$=44.49; p=0.0005; interaction $F_{(1,6)}$=1.157; p=0.3233). **C)** Time course of inactive lever pressing in D1- and D2-cre animals during heroin self-administration and extinction. No difference in inactive lever presses between rat genotype (effect of genotype $F_{(1,13)}$=1.071; p=0.3196), but significant effect of time ($F_{(19,\ 247)}$=5.673; p<0.0001); interaction ($F_{(1,\ 5)}$=1.842; p=0.0192). **D)** No difference in inactive lever presses during behavioral tests (2-way ANOVA; effect of genotype $F_{(1,6)}$=0.7328; p=0.4248; EXT/RST $F_{(1,6)}$=0.1397; p=0.7214; interaction $F_{(1,6)}$=0.1.658; p=0.2453). For RST data, each dot in bar represents an animal. **E,F)** No difference in total TIMP-1 and -2 expression across treatment groups between D1 and D2 MSNs (TIMP-1: 2-way ANOVA; effect of cell type, $F_{(1,\ 76)}$=3.646; p=0.0600; effect of group, $F_{(2,\ 76)}$=0.4607; p=0.6326; interaction, $F_{(2,\ 76)}$=0.1164; p=0.8903. TIMP-2: 2-way ANOVA; effect of cell type, $F_{(1,\ 75)}$=2.319; p=0.1320; effect of group, $F_{(2,\ 75)}$=1.219; p=0.3012; interaction, $F_{(2,\ 75)}$=1.039; p=0.2762.) Three to four image series were quantified per animal. Data are shown as mean ± SEM.

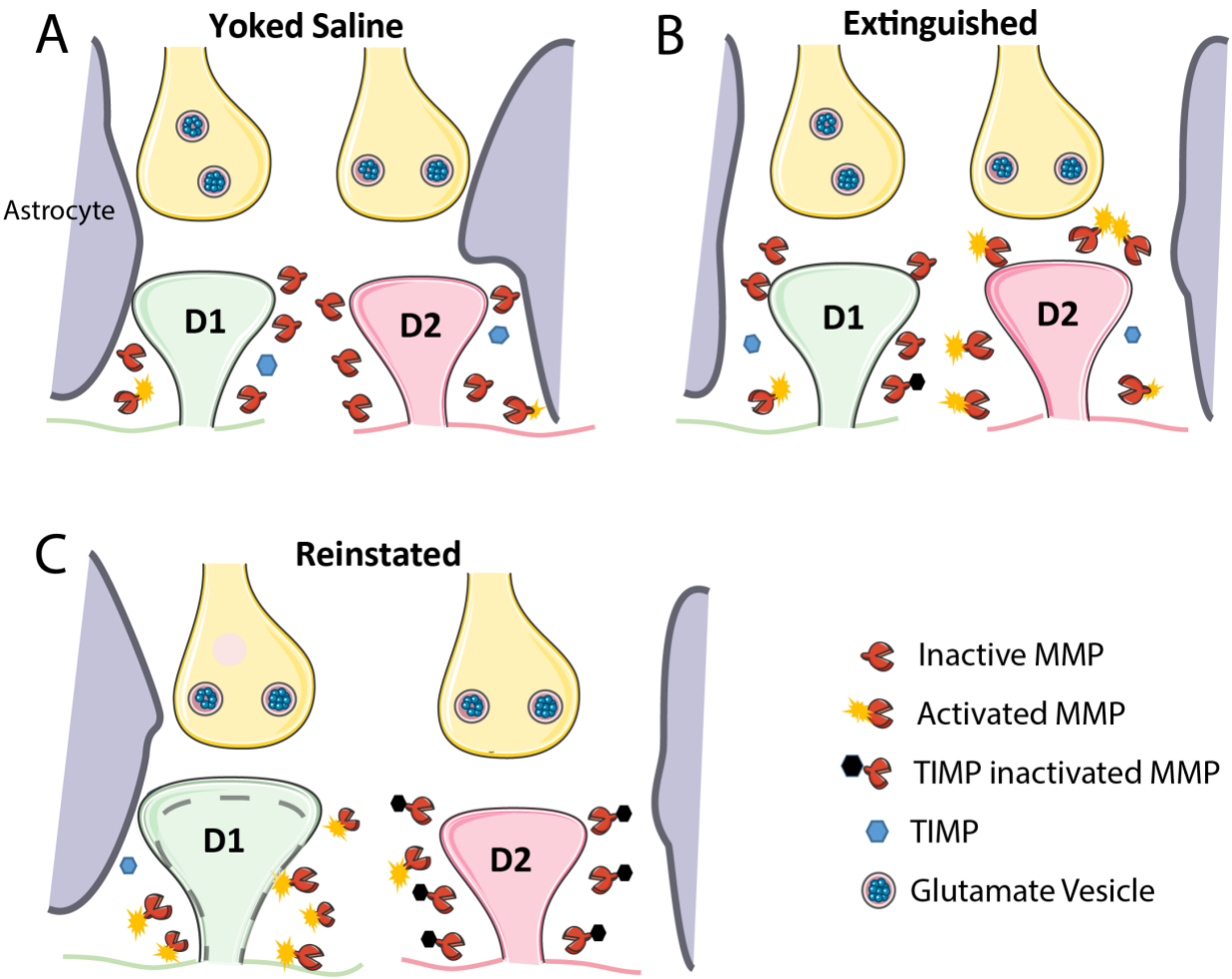

Supplemental Figure 8. Illustration depicting changes in MMP-2,9 activity around D1- and D2-MSNs and astroglia near the synapse during yoked saline control conditions, after extinction training and during cue-induced heroin seeking. A) Yoked saline controls show minimal activation of MMP and low levels of TIMP around MSN dendritic spines and synapse proximal astroglial protrusions. **B)** Extinction training activation MMP-2 selectively around D2-MSN dendrites, and increases in TIMP-2 around D1-MSNs reinforces MMP inactivity. **C)** Fifteen min of heroin cue-induced reinstatement astroglial protrusions return to the proximity of D1-MSN synapses, and D1-MSN spine heads enlarge. Heroin cues activate MMP-9 selectively around D1-MSN dendrites and increases in TIMP-1,2 around D2-MSNs inhibits extinction training induced MMP-2 activity. Presumed MMP-9 activity is also elevated around astroglia protrusions associated with D1-MSN synapses.

Supplemental Methods

Animals and Housing Care

Ninety-seven male and female Long Evans D1 and D2-Cre (+) transgenic rats (cre recombinase under control of the dopamine receptor D1 or D2 promoter; provided by National Institute of Drug Abuse; validated in (1) and 41 Cre (-) wildtype littermates, were individually housed using a 12:12 hr dark/light cycle with food and water made available ad libitum in a temperature and humidity-controlled environment. All experimentation occurred during the dark phase, and animals were allowed to acclimate to the vivarium environment for a week prior to surgery. All procedures were conducted in accordance with the NIH Guide for the Care and Use of Laboratory Animals and the Assessment and Accreditation of Laboratory Animal Care, and all measurements were made by an experimenter unaware of the animals treatment group.

Surgery: Catherization and Virus Transfection

Rats were ~60 days old (~250 g) when they were anesthetized with isoflurane (i.e. 5% concentration during induction, 2-3% concentration maintenance during surgery) before being implanted with indwelling jugular vein catheters, and received ketorolac (2 mg/kg, ip) as a pre-operative analgesic as well as the antibiotic cefazolin (10 mg/kg, ip). Following catherization, rats were stereotaxically implanted with bilateral guide cannulae (Plastics One Inc., 18-gauge) above the NAcore (1.5mm AP, 1.8mm ML, 5.5mm DV). Dummy injectors were placed in cannulae to maintain patency for future microinjections.

Immediately following guide cannula implantation, D1 and D2 medium spiny neurons were virally transfected with AAV1-EF1a-dflox-hChR2-mCherry (Addgene; 0.75 µL/hemisphere, 0.15 µL/min, 10-minute diffusion time). Additionally, in separate wildtype animals astroglia cells were selectively labeled using a glia fibrillary acidic protein (GFAP) promoter with AAV5-GFAP-hM3dq-mCherry (University of Zurich, Zurich, Switerland; 1.0 µL/hemisphere, 0.15 µL/min, 5-minute diffusion time). For experiments in this manuscript, ChR2 and hM3dq (Gq-coupled DREADD) were solely used for membrane-targeting of mCherry promoter and were not activated. Both viruses were injected in NAcore with 26-gauge microinjectors (Plastics One Inc.). Virus transfection occurred during surgery recovery and during the length of self-administration behavior (~4 weeks).

Drugs and reagents

Heroin HCl powder, provided by the National Institute of Drug Abuse, was dissolved in sterile normal saline. Both TIMP-1 and -2 antibodies (R&D Systems, #AF970 and #AF971, respectively) were utilized for their previously published capacities to inhibit TIMP-1 and -2 (2, 3). The working

dose of neutralizing antibody was a combination of equal parts of TIMP-1 (3 µg/ml) and TIMP-2 (3 µg/ml). This dose was selected based on neutralizing 50 (ND_{50}) values for both compounds (ND_{50}=1 µg/ml for TIMP-1 and ND_{50}=2.6 µg/ml for TIMP-2; obtained from product datasheet; R&D Systems). Normal Goat IgG (6 µg/ml) was used as a control reagent (R&D Systems, #AB-108-C). MMP-2i (Millipore-Sigma, #444288; 0.1 nmol; dissolved in 1% DMSO, IC_{50}=12 nM for MMP-2 and IC_{50}=0.2 µM for MMP-9 (4)). MMP-9i (Millipore-Sigma, #444278; 0.1 nmol; dissolved in 1% DMSO, IC_{50}=5 nM for MMP-9 (5)). Dye-quenched fluorescein conjugate gelatin (Thermo Fisher Scientific, #D12054; 1 mg/ml in phosphate buffered saline PBS; 1.5 µl/hemisphere) was used for *in vivo* zymography assay.

Heroin Self-administration, Withdrawal, and Cued Reinstatement

Rats underwent daily three-hour heroin self-administration sessions in two-lever operant chambers. Each active lever press delivered one 100 µg (days 1-2), 50 µg (days 3-4), or 25 µg (days 5-10) per IV infusion of heroin (FR1) paired with cues (light and tone) followed by a 20s timeout (Med Associates). The descending dosing protocol was used to facilitate the acquisition of heroin self-administration and to increase the number of active lever presses emitted by the end of self-administration training (6). Rats self-administered heroin for 10 days reaching criteria of ≥10 infusions/day on at least the last 3 days, followed by withdrawal (i.e. either extinction training or home-cage abstinence for 10 days). During extinction training, levers were presented and counted but did not trigger infusion of heroin or presentation of cues. Extinction proceeded for 10 training sessions or until rats reached the extinction criteria of ≤25 active lever presses for two consecutive days before a reinstatement test day. Home cage abstinence animals were handled and weighed daily and kept in behavioral room with operant chambers while their counterparts engaged in extinction training. This controlled for effects of daily handling. Tissue collection occurred either 24 hours after last day of extinction or abstinence or during a cued reinstatement test (15 or 120 mins) in which delivery of light and tone cues was restored to active lever pressing, but not heroin infusions. For one cohort of animals, after 10 days of extinction training, rats underwent “refraining” behavioral testing where rats were placed in extinguished operant chamber (15 mins) and no programmed consequences (i.e. cues or drug) were delivered with active lever pressing. Some experiments employed yoked-saline controls that were catheterized but received saline infusions in a randomized, noncontingent manner.

In vivo zymography

As demonstrated in previous work from our lab (7), *in vivo* zymography was utilized to assess changes in MMP function. Dye-quenched FITC-gelatin (Thermo Fisher Scientific) (reconstituted in PBS to 1 mg/mL, pH 7.2-7.4; 3.0µl of gel; 1.5µl/side) was microinjected, 2.0 mm beyond the

base of implanted guide cannula, with 15 min incubation time in home cage or the operant testing environment depending on the experiment group. Subsequently, an overdose of pentobarbital (3.9 mg/ml, ip) was administered and animals were transcardially perfused with 4% paraformaldehyde (PFA). Brains were removed, placed in 4% PFA overnight for additional fixation and a vibratome was used to obtain 100 µm sections, containing the injection track and anterior commissure (AC), through the NAcore. Sections were then either mounted and coverslipped or stained via immunohistochemistry (see below) and then subsequently imaged on a Leica SP5 (Wetzlar, Germany) or Carl Zeiss LSM 880 (Oberkochen, Germany) laser scanning confocal microscope. Only slices containing both the anterior commissure (landmark for NAcore) and injection site were imaged and analyzed by ImageJ software (NIMH, Bethesda, MD) (Figure 2a). Fluorescence was quantified bilaterally as integrated density from four-seven sections/rat. The integrated densities were averaged for each rat and normalized to yoked-saline control values.

Immunohistochemistry

Tissue sections were obtained as described above for zymography, and cell membranes were made porous using 1x PBS with 0.5% Triton-X-100 for 10 minutes at room temperature, then blocked with 1x PBS with 2% Triton-X-100 (PBST) with 2% normal goat serum for 45 minutes. Immunohistochemistry was conducted against the mCherry reporter protein to amplify virally-labeled D1 and D2 MSNs. Primary antibodies against mCherry (Rb anti-dsRed, 1:500; Takara #632496 or Mouse anti-mCherry, 1:1000; LSBio #204825) were incubated for 48 hours at 4˚C with gentle agitation. For detection of TIMP-1 and TIMP-2 expression, sections were incubated with monoclonal primary antibodies against TIMP-1 (1:500; Abcam #18352) and TIMP-2 (1:200; Thermo Fisher Scientific #12207). Tissue virally transfected with GFAP-mCherry virus to selectively label astrocytes were incubated with synapsin I antibody (1:1000; Abcam #64581) and mCherry was visualized without antibody amplification. Following incubation with primary antibodies, slices were washed with PBST and incubated overnight at room temperature in respective species-specific fluorescent secondary antibodies (Alexa Fluor; 1:1000; Thermo Fisher Scientific). After washing in PBST, slices were mounted and coverslipped using ProLong Gold Antifade Mountant (Thermo Fisher Scientific).

Confocal Microscopy Imaging

Z-stacks were acquired using a Leica SP5 or Carl Zeiss LSM 880 laser scanning confocal microscope equipped with Argon (Ar 488 nm), Helium-Neon (He-Ne 543 nm) or Helium-Neon (He-Ne 633 nm) laser lines.

Following quantification of MMP activity at low magnification (10x), 2 or 3 sections with the highest integrated density are selected for higher magnification single cell imaging. Dendritic segments

or astroglia are imaged ≤500 µm from the microinjector tip ("zymography zone"), with most images being collected between 250-500 µm due to frequent saturation of the fluorescent signal <250 µm from the injector tip (see Figure 2a). This range was selected due to majority of zymography signal being localized within this range, as well as slight differences in injector track orientation and virus expression throughout tissue section. As stated previously, cells were only imaged from brain sections containing both the microinjector track and anterior commissure in the frame to ensure that the individual cells being quantified were in NAcore.

Dendritic spine morphology image acquisition criteria were based on parameters previously described in (8). Only spiny dendrites located 75-200 µm from the soma and after the first branch point were imaged (see Figure 2b-d). Segment lengths were between 55-70 µm in length, and each dendrite segment was traced back to a different soma, thus there was one dendrite segment quantified per cell. Four to eight dendrites were imaged/animal at 63x using oil immersion objective lens at the following acquisition settings: 1024 x 256 frame size, 12-bit image resolution, 4-frame average, 0.21-µm step size, and digital zoom of 3.5x on Leica SP5 or 2.0x Carl Zeiss LSM 880 confocal microscope. Captured images were then deconvolved with Autoquant (Media Cybernetics, Rockville, MD) or processed with paired Zeiss Airyscan super-resolution deconvolution ZEN software. Following deconvolution, digital analysis of individual dendrites was processed using Imaris (version 8; Bitplane, MA) with three-dimensional (3D) space-filling Surface module to calculate % MMP gelatinolytic puncta localized within 300 nm of the dendrite surface. Final data set voxel dimensions were 0.0686 µm in the XY plane and 0.210 µm in the Z for Leica-acquired images, and 0.0659 µm in the XY plane and 0.210 µm in Z for Zeiss-acquired images.

Astrocytes were acquired at 63x using an oil immersion objective lens, 1024 x 1024 frame size, 12-bit image resolution, 4-frame averaging, 1-µm step size, and 1x digital zoom on Leica SP5. Three to eight astrocytes were imaged/animal. Acquired images were iteratively deconvolved 10 times (Autoquant) and digital analysis of mCherry signal intensity relative to background was used to generate a digital model of each astrocyte and corresponding extracellular MMP activity (Bitplane Imaris). All imaging and analyses were conducted by investigator blind to animal treatment groups.

The first experiments conducted are shown in figures 3 (SAL, EXT, and RST 15' groups), 4 and 6, were performed using Leica SP5 confocal. Subsequent experiments shown in figures 3 (ABS, REF 15, and RST 120' groups), 5, 7, and 8 were imaged using Zeiss confocal.

<u>Imaris 3D Reconstruction, Morphological Analyses and Colocalization Quantification</u>

The following sections describe quantification methodology utilizing Imaris software analysis (see Figure 2a-g for illustration). All analyses were conducted by investigators blind to animal treatment groups.

Imaris 3D Processing: D1/D2 MSN MMP Activity Localization

Using Imaris Surface module, mCherry-labeled dendritic segments were cropped and isolated from background. The regions surrounding the dendrites was used to mask MMP-2,9 gelatinolytic puncta localized only within 300 nm from the surface of each labeled dendritic segment (i.e. total extracellular activity). This cutoff was established due to the limit of lateral and axial resolution for confocal microscopy using Leica SP5, which is approximately 250 and 500 nm, respectively, and 140 and 400 nm, respectively, using Zeiss LSM 880 (9). Gelatinolytic puncta were isolated by semi-automatic, intensity-based thresholding in order to isolate active MMP-2,9 puncta located around region of interest surrounding the dendritic segment (≤ 300 nm) (Figure 2e-g). MMP gelatinolytic activity localized adjacent to the dendrite was calculated by dividing volume (μm^3) of MMP puncta by volume (μm^3) of 300 nm-expanded region around dendrite to obtain normalized index of MMP activity around an isolated dendrite (MMP activity, % vol) (Figure 2g). This same approach was employed for quantification of extracellular TIMP-1,2 expression around virally labeled D1 and D2 MSNs.

In subsequent experiments described in Results section, dendritic spine head diameter was calculated for isolated mCherry-labeled dendrites previously quantified for % MMP activity adjacent to dendrite surface. The Filament module was used to semi-automatically trace dendritic shaft and identified dendritic spines as described previously (10). Spine head diameter was calculated using an automated threshold set by Imaris.

Once filament tracing was completed with the filament module, the “filament analysis” extension was used to create dendritic subcompartments. Once generated, these regions were then uniformly expanded by 300nm in all directions, to create the regions of interest required to then determine the extent of MMP-2,9 puncta localized around dendritic spine heads or the dendritic shaft with Imaris software. All MMP-2,9 puncta not corresponding to signal within the expanded regions of interest were eliminated in order to isolate only signal around the spine head or shaft (10). MMP signal accumulation calculated as described above for 1) spine head-specific and 2) shaft-specific MMP puncta by normalizing volume of compartment-specific MMP signal in μm^3 (i.e. spine head or shaft) to volume of 300 nm-expanded region around the specific dendritic subcompartment of interest (Figure 2g, 3). The spine head:shaft ratio was also determined by dividing the score for MMP puncta signal around each respective compartment.

Imaris 3D Processing: Astroglial Morphology and MMP Activity Co-localization

The digital astroglial model generated from the hM3Dq-mCherry signal was generated as described in detail by (11, 12) and used to mask out MMP-2,9 activity and Synapsin I signal that were not co-registered with the astroglial volume. Co-localization (astrocyte with Synapsin I, astrocyte with MMP-2,9 puncta, MMP-2,9 puncta with Synapsin I) was determined based on thresholded signal intensity in each channel. Voxels containing fluorescent signal intensity greater than noise in each channel were determined empirically by an investigator blinded to the treatment group within the colocalization module and were used to build a colocalization channel. The Imaris Surface Module was used to measure the colocalization channel characteristics, including net volume of colocalized signal. Synapsin and MMP-2,9 puncta colocalization were normalized to the volume of the astrocyte from which they were generated. Surface-proximal MMP-2,9 puncta were determined by excluding colocalized signal >250nm from the astrocyte and was normalized to total MMP-2,9 puncta from the same astroglial volume.

Statistical analysis

All statistical analyses were conducted in GraphPad software (Prism v 8). Behavioral data were analyzed by two-way ANOVA followed by Bonferroni post hoc tests for multiple comparisons. D'Agostino-Pearson normality test was used to determine if data were normally distributed. Kruskal-Wallis with Dunn's post hoc comparisons or Mann-Whitney tests were used when one or more treatment groups in an experiment were found to be not normally distributed. Data found to be normally distribution were analyzed using a one- or two-way ANOVA. When two groups were compared, a two-tailed paired or unpaired Student's t-test was utilized. All D1/D2 cell-specific data was analyzed using either Nested t-test (two group comparison) or Nested ANOVA with post-hoc Bonferroni analysis when significant interaction was observed (multiple group comparison). In all cases, p values <0.05 were considered significant. All data except behavior was collected and quantified by investigators blind to animal treatment groups.

References

1. Garcia-Keller C, Scofield M, Neuhofer D, Varanaxi S, Anderson E, Richie CT, et al. (2020): Relapse-associated transient synaptic plasticity requires integrin-mediated activation of focal adhesion kinase and cofilin. *Journal of Neuroscience*. in press.

2. Reikvam H, Hatfield KJ, Øyan AM, Kalland KH, Kittang AO, Bruserud Ø (2010): Primary human acute myelogenous leukemia cells release matrix metalloproteases and their inhibitors: release profile and pharmacological modulation. *European Journal of Haematology*. 84:239-251.

3. Lu D, Liao Y, Zhu S-H, Chen Q-C, Xie D-M, Liao J-J, et al. (2019): Bone-derived Nestin-positive mesenchymal stem cells improve cardiac function via recruiting cardiac endothelial cells after myocardial infarction. *Stem Cell Res Ther*. 10:127-127.

4. Rossello A, Nuti E, Orlandini E, Carelli P, Rapposelli S, Macchia M, et al. (2004): New N-arylsulfonyl-N-alkoxyaminoacetohydroxamic acids as selective inhibitors of gelatinase A (MMP-2). *Bioorganic & Medicinal Chemistry*. 12:2441-2450.

5. Levin JI, Chen J, Du M, Hogan M, Kincaid S, Nelson FC, et al. (2001): The discovery of anthranilic acid-Based MMP inhibitors. Part 2: SAR of the 5-position and P11 groups. *Bioorganic & Medicinal Chemistry Letters*. 11:2189-2192.

6. Zhou W, Kalivas PW (2008): N-acetylcysteine reduces extinction responding and induces enduring reductions in cue- and heroin-induced drug-seeking. *Biological psychiatry*. 63:338-340.

7. Smith AC, Kupchik YM, Scofield MD, Gipson CD, Wiggins A, Thomas CA, et al. (2014): Synaptic plasticity mediating cocaine relapse requires matrix metalloproteinases. *Nat Neurosci*. 17:1655-1657.

8. Shen H, Sesack SR, Toda S, Kalivas PW (2008): Automated quantification of dendritic spine density and spine head diameter in medium spiny neurons of the nucleus accumbens. *Brain Structure and Function*. 213:149-157.

9. Schermelleh L, Heintzmann R, Leonhardt H (2010): A guide to super-resolution fluorescence microscopy. *J Cell Biol*. 190:165-175.

10. Siemsen BM, Giannotti G, McFaddin JA, Scofield MD, McGinty JF (2019): Biphasic effect of abstinence duration following cocaine self-administration on spine morphology and plasticity-related proteins in prelimbic cortical neurons projecting to the nucleus accumbens core. *Brain Struct Funct*. 224:741-758.

11. Kruyer A, Scofield MD, Wood D, Reissner KJ, Kalivas PW (2019): Heroin Cue–Evoked Astrocytic Structural Plasticity at Nucleus Accumbens Synapses Inhibits Heroin Seeking. *Biological Psychiatry*. 86:811-819.

12. Scofield MD, Li H, Siemsen BM, Healey KL, Tran PK, Woronoff N, et al. (2016): Cocaine Self-Administration and Extinction Leads to Reduced Glial Fibrillary Acidic Protein Expression and

Morphometric Features of Astrocytes in the Nucleus Accumbens Core. *Biol Psychiatry*. 80:207-215.